Anal Bioanal Chem (2012) 403:419–430
DOI 10.1007/s00216-012-5879-9

ORIGINAL PAPER

Pyrolysis and combustion of tobacco in a cigarette smoking simulator under air and nitrogen atmosphere

Christian Busch · Thorsten Streibel · Chuan Liu · Kevin G. McAdam · Ralf Zimmermann

Received: 21 December 2011 / Revised: 10 February 2012 / Accepted: 14 February 2012 / Published online: 6 March 2012

Abstract A coupling between a cigarette smoking simulator and a time-of-flight mass spectrometer was constructed to allow investigation of tobacco smoke formation under simulated burning conditions. The cigarette smoking simulator is designed to burn a sample in close approximation to the conditions experienced by a lit cigarette. The apparatus also permits conditions outside those of normal cigarette burning to be investigated for mechanistic understanding purposes. It allows control of parameters such as smouldering and puff temperatures, as well as combustion rate and puffing volume. In this study, the system enabled examination of the effects of "smoking" a cigarette under a nitrogen atmosphere. Time-of-flight mass spectrometry combined with a soft ionisation technique is expedient to analyse complex mixtures such as tobacco smoke with a high time resolution. The objective of the study was to separate pyrolysis from combustion processes to reveal the formation mechanism of several selected toxicants. A purposely designed adapter, with no measurable dead volume or memory effects, enables the analysis of pyrolysis and combustion gases from tobacco and tobacco products (e.g. 3R4F reference cigarette) with minimum aging. The combined system demonstrates clear distinctions between smoke composition found under air and nitrogen smoking atmospheres based on the corresponding mass spectra and visualisations using principal component analysis.

Keywords Single-photon ionisation · Mass spectrometry · Pyrolysis · Cigarette mainstream smoke · Tobacco · 3R4F

C. Busch · T. Streibel (✉) · R. Zimmermann
Joint Mass Spectrometry Centre, Chair of Analytical Chemistry, Institute of Chemistry, University of Rostock, 18057 Rostock, Germany
e-mail: Thorsten.Streibel@uni-rostock.de

C. Liu · K. G. McAdam
Group Research and Development Centre, British American Tobacco, Southampton SO15 8TL, UK

T. Streibel · R. Zimmermann
Joint Mass Spectrometry Centre, Cooperation Group "Analysis of Complex Molecular Systems," Institute of Ecological Chemistry, Helmholtz Zentrum München–German Research Centre for Environmental Health, 85764 Neuherberg, Germany

Introduction

Pyrolysis experiments offer the possibility of unravelling mechanistic information about the complex processes involved in the thermal decomposition of biomass materials. This has been demonstrated by investigating single components, such as glycerine or D-glucose [1–4], biopolymers, such as cellulose, lignin or pectin [5, 6], and more complex types of biomass, such as hardwood or softwood [7, 8]. Another biomass of great interest is tobacco because its use in the form of cigarettes involves the generation of various smoke compounds from combustion and pyrolysis reactions [9, 10].

Most analytical methods concerning cigarette smoke chemistry employ the trapping and separation of a smoke aerosol stream (e.g. filter pads, impinger, absorbent tubes) at the end of a smoking process, with any results so obtained reflecting the whole cigarette smoking process [11, 12]. This leads to averaged information about the progress of substance formation during the smoking process that cannot reveal information about their detailed reaction mechanisms. Other techniques may be adapted to analyse tobacco smoke on a puff-resolved basis including chemical ionisation mass

spectrometry [13], multiplex gas chromatography-mass spectrometry [14, 15], liquid chromatography electrospray ionisation tandem mass spectrometry [16] and extraction and derivatisation in single drop coupled to matrix-assisted laser desorption/ionisation Fourier transform ion cyclotron resonance mass spectrometry [17]. In other works, selected compounds in a single puff have been monitored online by Fourier transform infrared spectroscopy [18, 19], quad quantum cascade laser spectrometry [20, 21], quantum cascade tuneable infrared laser differential absorption spectroscopy [22] and lead-salt tuneable diode laser infrared spectroscopy [23]. The limitations of these techniques are their relatively low time resolution and their specialisation in a few selected compounds such as carbon dioxide [21], acrolein or 1,3-butadiene [23]. Since tobacco smoke is a complex and reactive matrix containing over 5,600 identified compounds in vapour and particle phases [11, 24, 25], unravelling mechanistic information in real time requires a fast analysis technique. Time-of-flight mass spectrometry combined with photo ionisation has been proven to be capable of analysing cigarette smoke and other complex gas mixtures online with a high time resolution [10, 26–35]. Various volatile organic compounds covering a wide dynamic range of concentrations can be detected. Photo ionisation includes two different ionisation mechanisms: single-photon ionisation (SPI) and resonance enhanced multi-photon ionisation (REMPI). The results described in this work refer to the application of single-photon emission–time-of-flight mass spectrometry (SPI-TOFMS). Vacuum ultraviolet (VUV) photons with a wavelength of 118 nm are used to generate ions in a single step without forming fragments. The type of substances that can be detected include aromatics (e.g. benzene), aliphatics (e.g. 1,3-butadiene), heterocyclic compounds (e.g. pyridine) and carbonyl compounds (e.g. acetaldehyde). The detection of bulk matrix compounds present in the combustion atmosphere such as nitrogen, oxygen, water and carbon dioxide is suppressed due to their ionisation potentials exceeding the energy of the laser-generated VUV-photons [10, 28].

This work reports some initial results on the formation processes of selected smoke compounds using a cigarette smoking simulator. The heat needed to burn a cigarette under simulated puffing and smouldering conditions is provided externally by three 150 W infrared (IR)-lamps located inside the cigarette smoking simulator. This feature enables the possibility of "smoking" a cigarette under normal conditions (air atmosphere) as well as under inert conditions (nitrogen atmosphere). This unique technique avoids a major disadvantage of other pyrolysis experiments, which are usually carried out in a micro-furnace. This makes the detection of trace compounds challenging due to the small amount of sample burnt and the lack of adequate filtration. Mass transport steps are indispensable key features for effectively approximating the real smoke formation steps in a cigarette. After smoke is generated via drying, distillation, pyrolysis and combustion processes, its composition is changed by filtration (tobacco rod and cigarette filter) and chemical reactions [36]. Therefore, the composition of the smoke exiting a cigarette is dependent on several parameters operating in a real cigarette which have to be simulated by the cigarette smoking simulator if possible.

The present work describes the utilisation of SPI-TOFMS combined with a cigarette smoking simulator for the analysis of simulated mainstream smoke of a Kentucky 3R4F research reference cigarettes, obtained under either oxidative or inert conditions, with an intra-puff time resolution of 0.1 s. The substances recorded cover from *m/z* 17 (ammonia) to *m/z* 162 (nicotine). The objective of this research is to establish any changes of the major species when the atmosphere is switched from air to nitrogen.

Experimental section

Laser-SPI-TOFMS

The setup of the SPI-TOFMS system has already been described in detail before [27, 37], therefore only a brief description is given below.

VUV photons are generated by Nd:YAG laser pulses (Surelite-III, Continuum, Santa Clara, USA; λ=1064 nm, ν=10 Hz, t_{plus}=5 ns). First, UV photons (λ=355 nm, P=128 mW) are induced by triplication of the Nd:YAG fundamental via a third harmonic generator. Afterwards, a second triplication process in a xenon gas cell (Xe 4.0; p=12 mbar) is used to generate the VUV photons (λ=118 nm, E=10.49 eV). Their energy is sufficient to ionise substances featuring an ionisation potential equal to or less than 10.49 eV in a single step (SPI).

Cigarette smoking simulator

The cigarette smoking simulator (C-Matic Systems, UK) was designed to simulate the main thermophysical processes occurring during cigarette smoking. The simulator consists of three main parts: a microprocessor controller unit, a housed combustion fixture and a modified A14 syringe driver (Borgwaldt KC, Germany). The controller unit regulates the chosen parameters, such as the set temperature of the three IR-lamps to cover the selected puff and smoulder temperatures, tube movement speed that is equivalent to the linear burn rate of a conventional cigarette, backflow gas purging rate and puffing flow volume. The combustion fixture contains a Cambridge filter pad holder, which can be used to hold a cigarette or a quartz tube loaded with a known amount of tobacco sample. It also has a connection port linking to the A14 syringe driver on a moveable shuttle. An accurate stepper motor moves the quartz tube into the focal point of the three IR-lamps and also

delivers the pre-selected puffing and smouldering burn rates. The volume of the tobacco rod being heated is approximately the same as that of a conventional burning tip of a cigarette.

Sample materials

All experiments were carried out using 3R4F Kentucky research reference cigarettes (University of Kentucky, USA). They deliver 9.4 mg tar, 0.73 mg nicotine and 12.0 mg carbon monoxide under ISO/FTC machine-smoking conditions [38]. Detailed smoke chemistry yields from these cigarettes have been examined by two separate interlaboratory test studies [39, 40]. Whole 3R4F cigarettes were inserted directly inside the quartz tube and burnt without modification. The cigarettes were stored for several days in an air-conditioned room at 22 °C prior to their usage.

Simulated smoking under nitrogen atmosphere

A schematic representation of the two different operating states for measurements under nitrogen atmosphere is shown in Fig. 1. The pathways for smoke and nitrogen during the puffing phase are displayed by dashed arrows and solid arrows during the smouldering phase, respectively. If nitrogen is mixed with smoke, the arrows are dark grey.

Prior to each measurement, the quartz tube loaded with a 3R4F cigarette was purged with nitrogen for 30 s to remove air from the void volume of the tobacco rod and the cigarette filter. An excess of nitrogen ((1a) and (1b)) flows through the T-piece (shown on the left hand side) constantly during operation. During a puff, a volume of 35 ml nitrogen is drawn over 2 s and repeated once every 60 s [41] by the syringe driver (5a) and passes through the quartz tube and the cigarette (2a). When the lamp power is increased from smouldering to puffing, the temperature of the burning tobacco in the focal point raises immediately to the set point; in this work, it is set at 900 °C. This temperature corresponds to the mean temperature of a normal burning cigarette during puffing [42–44]. The shuttle speed increases simultaneously at the start of the puff to 120 mm/min to simulate the higher linear burning rate during a puff [45]. The pyrolysis products are carried over to the adapter, and a small fraction of this effluent (flow rate=5 ml/min) is drawn through the sampling capillary inside the heated transfer line (T=280 °C) and fed into the mass spectrometer. Inside the ion source of the mass spectrometer, the smoke compounds are ionised by VUV-pulses, and the formed molecular ions are subsequently separated according to their time of flight, which is then converted into mass-to-charge (m/z) ratios.

At the end of the puff, the syringe driver valve is closed (4b) and the backflow valve is opened (5b) to allow the effluents (e.g. water and volatile compounds) generated during smouldering burn to be taken out the tube from the opposite direction to the mainstream smoke. This nitrogen purges (at the back flow rate=17.5 ml/min) the adapter and also the capillary inside the heating hose (3b). During the entire smouldering phase, the shuttle speed decreases to 5 mm/min [46, 47], and the lamp power is lowered to allow a smouldering temperature of 600 °C (surface smouldering temperature for a conventional burning cigarette=675 °C [48]).

Experiments with an air atmosphere are carried out in a similar way but with two exceptions. The fume hood is brought near to the quartz tube without the T-piece connection, i.e. open to the ambient air, and the back flow is connected to a

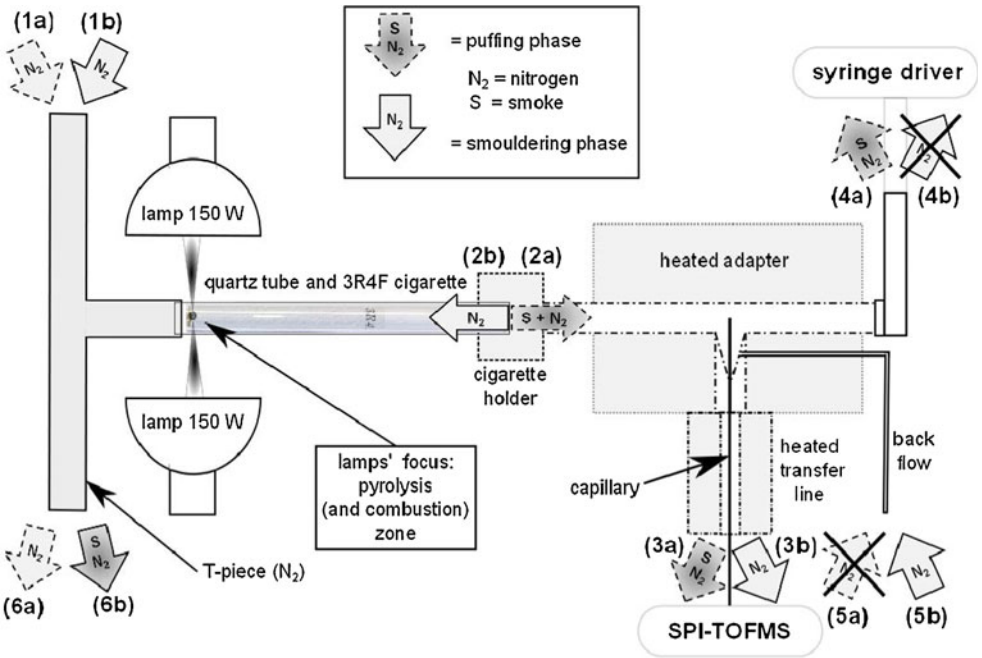

Fig. 1 Schematic representation of cigarette smoking simulator combined with adapter to mass spectrometer: (*1a*)-(*6a*) puffing phase, (*1b*)-(*6b*) smouldering phase [(*1a*) nitrogen supply, (*2a*) smoke generation in the lamps' focus and mixing with nitrogen, (*3a*) smoke analysis, (*4a*) drawing (35 ml over 2 s every 60 s), (*5a*) no backflow supply, (*6a*) fraction of nitrogen excess; (*1b*) nitrogen supply, (*2b*) and (*3b*) nitrogen purging, (*4b*) no drawing, (*5b*) nitrogen backflow supply, (*6b*) smoke and purging gas]

supply of pressurised and cleaned laboratory air, supplied at the same backflow rate of 17.5 ml/min.

Connection between MS and cigarette smoking simulator

The adapter linking the simulator and the mass spectrometer plays a critically important role.

However, it ensures a sufficient purging of itself and the transfer line immediately post-puffing, thus the MS-signal was reached 2 to 3 s after the puff was finished, as shown in Fig. 2 for isoprene and benzene. The remaining time (2 to 3 s) after the 2 s puff shows the purging behaviour of the adapter and transfer line.

Data evaluation

The signals (intensity as a function of time-of-flight) recorded were mass-calibrated and exported as ASCII data file by a customised LabVIEW-based (National Instruments, USA) software for further evaluations in Origin 8.1 (OriginLab, USA) and The Unscrambler v9.7 (Camo Software AS, Norway).

The results obtained in this work are based on mean values from puff number 2 to 6, and the puffing parameters used are 35 ml puff volume, 2 s duration and once every 60 s (i.e. the ISO puff parameters [41]). The yield from each puff was averaged over 2 s, i.e. the period from the puffs beginning to the end which corresponds to 20 single mass spectra. Ten replicates under each atmospheric condition, i.e. nitrogen and air atmosphere, were measured, and the mean values including the associated standard deviations were calculated. For further statistical evaluations, 39 assignable masses with the highest signal intensities were selected and summarised in Table 1.

The analysis technique did not allow the differentiation of isobars, thus the mass assignment in this work was carried out by relating the mass (*m/z*) to known tobacco smoke compounds which are accessible by SPI-TOFMS [49]. For selected isobaric compounds (e.g. *m/z* 56, *m/z* 58 and *m/z* 68), it is also possible to determine the predominant compound [50]. Partially, compounds' names concerning a certain mass are omitted.

The first puff was excluded because of the unique ignition of the cigarette, i.e. the cigarette was lit from a radial direction rather than from the front end as a conventional cigarette. The last puff was excluded because of the closeness of the heating with respect to the cigarette filter, which may be able to desorb some condensed semi-volatile compounds from the cigarette filter.

For further statistical analysis of the data sets, principal component analysis (PCA) was utilised. PCA attempts to identify interdependencies between key features within complex data sets. New artificial variables, viz. the principal components are formed and arranged in an ascending order to statistically account for most of the variance of the original data set [51, 52]. Each of the signal intensities (SI) of the 39 selected masses were normalised to the maximum: SI_{max}(nitrogen and/or air)=1. This normalisation method suppresses the influence of substances with high concentrations in tobacco smoke towards substances with low concentrations and emphasises their different behaviour based on the varying external experimental conditions. All input variables were pre-processed by mean centring (i.e. subtraction of the mean value from each value of one feature (here, *m/z*)) to translate the centre of the data cloud to the origin of the score plot to allow an easier interpretation of the PCA-results.

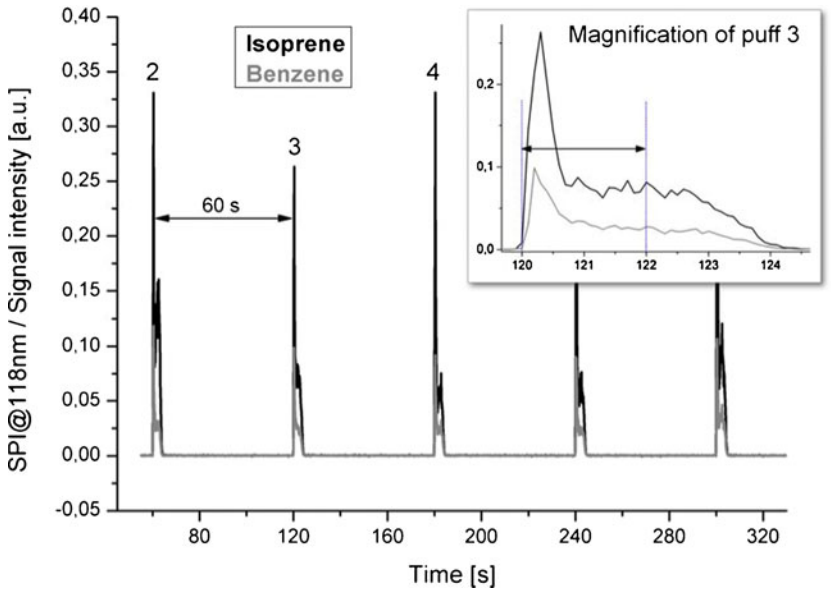

Fig. 2 Signal intensity of isoprene (*black*) and benzene (*grey*) of one 3R4F cigarette by using theoptimised adapter between cigarette smoking simulator and mass spectrometer (puff number 2 to 6)

Table 1 Selected 39 compounds based on their signal intensities and their potential appearance in tobacco smoke [11, 31, 53, 54]

m/z	Substances
17	Ammonia (NH_3)
30	Nitrogen monoxide (NO)
34	Hydrogen sulphide (H_2S)
40	Propyne
42	Propene
43	Carbohydrate fragment: $C_3H_7^+$, $C_2H_3O^+$
44	Acetaldehyde
48	Methanethiol
54	1,3-Butadiene, 1-butyne
56	1-Butene, 2-propenal
57	Carbohydrate fragment, 2-propen-1-amine
58	Acetone, propanal
66	Cyclopentadiene
67	Pyrrole
68	Isoprene, furan, 1,3-pentadiene, cyclopentene
69	Pyrroline
70	2-Butenal, pentenes
72	2-Methylpropenal, 2-butanone, butanal
78	Benzene
79	Pyridine
80	Pyrazine
81	Methylpyrrole
82	Methylfuran, methylcyclopentene, cyclohexane, 2-cyclopenten-1-one
84	Nicotine fragment, hexenes
85	Methylpyrrolidine, piperidine
86	Methylbutanal, pentanone
92	Toluene
93	Aniline, methylpyridine
94	Phenol
95	Pyridinol, dimethylpyrrol
96	Dimethylfuran, furfural
104	Styrene
106	Xylenes, benzaldehyde
107	Ethylpyridine, 3-pyridinecarboxaldehyde
108	Anisol, methylphenols
110	Dihydroxybenzenes, methylfurfural
120	C_3-Alkylbenzenes, phenylacetaldehyde, acetophenone
136	Limonene, methoxybenzaldehyde
145	2-(4-Pyridyl)furan, 2,3-dimethyl-1H-indole, 3-ethylindole

Results

An initial assessment of the cigarette smoking simulator's suitability to reproduce chemistry from mainstream cigarette smoke was carried out by comparing selected volatile and aerosol species present in the mainstream cigarette smoke. In the smoking simulator, for a given linear burning rate, the burning conditions are determined by the set smouldering and puffing temperatures and puffing conditions. The missing ventilation leads only to a lower smoke dilution and a higher compound concentration which should have a proportional effect on the chemical composition of the smoke. Hence, similar but not equal relative profiles of main chemical species are expected from the cigarette smoking simulator and from burning cigarettes. The first comparison was done with the results obtained for this work (i.e. cigarette smoking simulator, 3R4F cigarettes), a different measurement series (3R4F cigarettes, smoking machine) and another previously published measurement using SPI-TOFMS with 2R4F cigarettes [55] (a predecessor of the 3R4F) and a smoking machine [34]. Figure 3a shows the signal intensities of seven compounds normalised to the highest peak, viz. acetaldehyde for all measurements. Comparison of the signal intensity ratios between the three experiments shows quantitative differences across a number of compounds, but broad directional similarities in the trends between the ratio profiles found with different compounds. The second comparison was done with a high-performance liquid chromatography (HPLC) analysis of carbonyl compounds using the smoking simulator and a standard smoking machine (according to the ISO puffing parameters). Figure 3b shows the sum of mainstream smoke yields from eight carbonyl compounds provided by the two devices with single-grade Virginia and Burley tobacco experimental cigarettes. The features of these experimental cigarettes can be found in Adam et al. [30]. The yields generated by the simulator are higher due to the absence of filter ventilation and paper permeability. Again, the relative ratio of most analytes (exception for acetone) between the two tobacco types can be reproduced by the smoking simulator (Fig. 3c). This degree of conformity enables analysis of smoke chemistry reactions from burning tobacco in the cigarette smoking simulator to provide insights into the thermochemistry of tobacco within a burning cigarette.

Two averaged mass spectra of the fourth puff measured under nitrogen and air atmosphere, respectively, are shown in Fig. 4. The pattern of the mass spectrum (air atmosphere) is comparable to a mass spectrum of the fourth puff from a puff-resolved analysis of 2R4F reference cigarettes reported previously in Adam et al. [34]. Both mass spectra in Fig. 4 appear to be very similar. For example, the patterns concerning the five highest signal intensities of *m/z* 44 (acetaldehyde), *m/z* 68 (isoprene), *m/z* 58 (acetone), *m/z* 42 (propene), *m/z* 92 (toluene) and *m/z* 56 (butene) are visually equal. One obvious

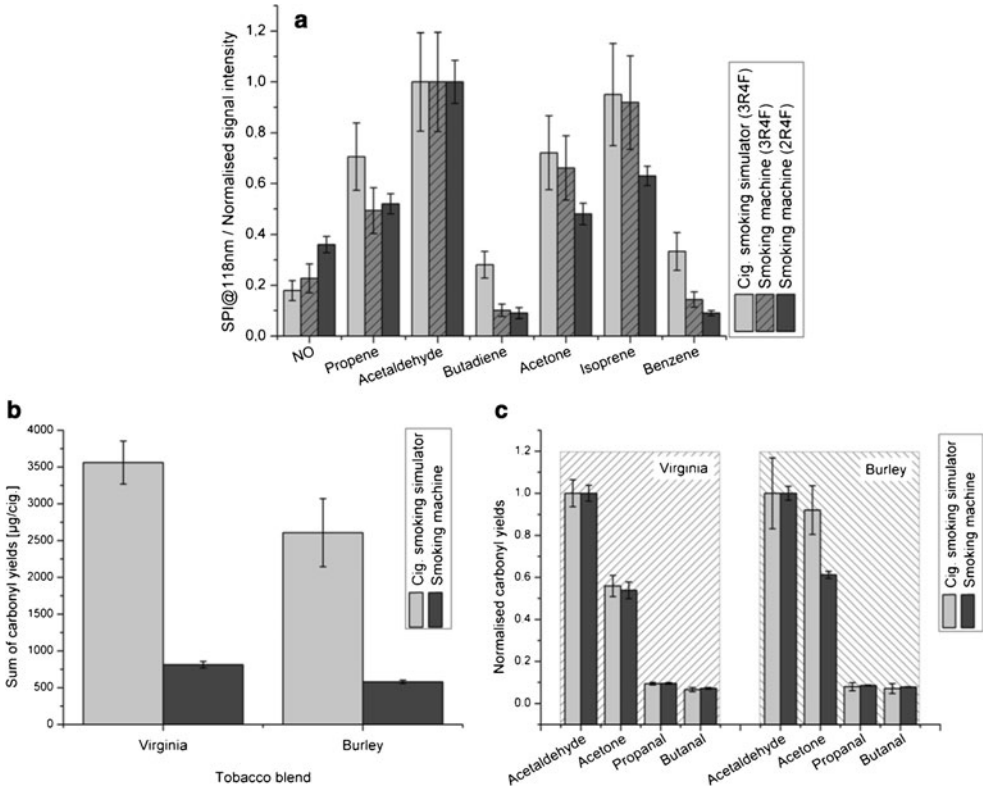

Fig. 3 **a** Normalised signal intensities (acetaldehyde intensities=1) of selected compounds from the fourth puff of 3R4F (cigarette smoking simulator), of 3R4F (smoking machine) and of 2R4F cigarettes (smoking machine) (SPI-TOFMS, n=10); **b** sum of carbonyl compounds' (formaldehyde, acetaldehyde, acetone, acrolein, propanal, crotonaldehyde, butanone and butanal) smoke yields (HPLC-UV, n=3); **c** normalised individual smoke yields (acetaldehyde yields=1) from the cigarette smoking simulator and a smoking machine of two single tobacco types (HPLC-UV, n=3)

difference between the two experimental conditions is the higher signal intensity of nearly all the mass-to-charge ratios measured under nitrogen atmosphere. The following statistical evaluations will emphasize the major differences of the atmosphere change.

The PCA score plot, shown in Fig. 5a, features the distinction of the experimental parameters (puff number and gas atmosphere, respectively). Principal component 1 (PC1) explains 62% of the total variance of the data set and separates the experiments mainly by the gas atmosphere. PC2 explains 24% of the total variance and separates the experiments due to the puff number. The experimental parameters cannot assigned completely to a single principal component, thus a new coordinate system (grey dashed arrows, rotated anti-clockwise through 45°) is applied to the score and loading plot. The new coordinate system separates the different features more clearly. The influence of the variables and their linkage to the calculated model is presented in the loading plot in Fig. 5b and the magnified section in Fig. 5c. Five compounds stand out noticeably from the bulk near the point of origin: ammonia (*m/z* 17), 2-(4-pyridyl)furan/2,3-dimethyl-1H-indole/3-ethylindole (*m/z* 145), hydrogen sulphide (*m/z* 34), dihydroxybenzene (*m/z* 110) and methylpyrrolidine/piperidine (*m/z* 85). These compounds are marked by grey frames in Fig. 5b and have the strongest influence on the PCA model. Figure 6 shows the mean signal intensities of eight selected compounds featuring a more or less noticeable difference between the yields generated under different conditions (atmosphere, puff number).

Given a certain tobacco blend, ammonia content in the mainstream smoke is strongly influenced by puff number as shown by these results (high values for PC1 and PC2, Fig. 5b), i.e. its concentration rises with increasing puff number. In addition, ammonia (Fig. 6a) possesses a different puff dependency compared with pyrrole (Fig. 6b). Ammonia's signal intensity increases more sharply from puff 6 than that of pyrrole under both atmospheres. In a previous work [30], a similar exponential increase in ammonia yield was found for a Burley tobacco cigarette but not for the 2R4F reference cigarette. Two other previous works [56, 57] describe the significant increase of ammonia release on a puff-by-puff basis from a 1R4F reference cigarette (i.e. the predecessor of the 2R4F reference cigarette). A similar puff-by-puff increase of pyrrole was also reported [37].

Hydrogen sulphide possesses the maximum value for PC1 and is therefore located between the new artificial axes. Hydrogen sulphide (Fig. 6c) yields show a strong puff dependency [34] and additionally a strong atmospheric dependency. It features a low signal during the second puffs compared with the later puffs and a larger signal difference between the two atmospheres whereas methanethiol (Fig. 6d) shows no puff dependency and a less distinctive difference due to the atmosphere change.

Another two compounds are located in the negative area of the loading plot (Fig. 5b) and also excluded from the

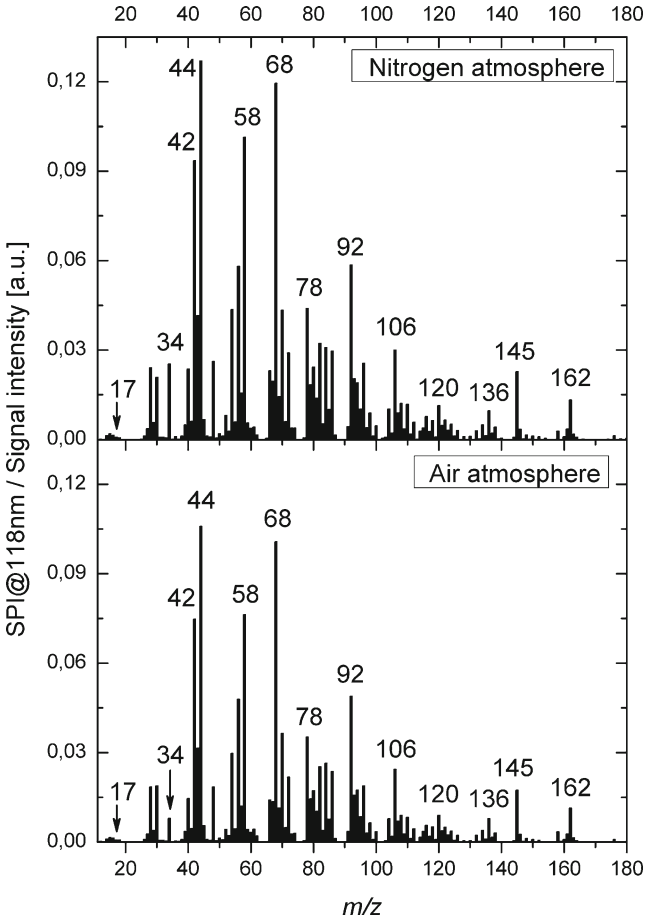

Fig. 4 Mean mass spectra of puff number 4 from ten 3R4F cigarettes smoked under nitrogen and air atmosphere (based on ISO puffing conditions)

compact group located near the axes' intercept point: dihydroxybenzene (*m/z* 110) and methylpyrrolidine/piperidine (*m/z* 85). These compounds (Fig. 6e, g) exhibit a strong puff dependency, although in the opposite manner to that of ammonia, i.e. a signal decrease with increasing puff number. The puff-by-puff decreasing trend for dihydroxybenzene is different from that of conventionally smoked 2R4F cigarettes where the amount increases as the puff number increases [37]. The profile of the phenol's signal (Fig. 6f) shows no significant differences between the atmospheres and a weak puff dependency, which agrees with a previous work [37].

The yield of 2,3-dimethyl-1H-indole/2-(4-pyridyl)furan/3-ethylindol (*m/z* 145) is also determined by the puff number and shows a similar behaviour to that of hydrogen sulphide (Fig. 6h). The maximum yield is reached after the third puff, thus these compounds feature lower values for PC1 and PC2 in Fig. 5b compared with ammonia.

To extract further information from the compact group of compounds, this area has been magnified in Fig. 5c. Substances such as phenol (*m/z* 94) and benzene (*m/z* 78) featuring values (for PC1 and PC2) close to zero on the left-hand side of this section are not influenced by the experimental parameters. Nitrogen-containing and heteroaromatic compounds, at the top right of this section such as pyridine (*m/z* 79) and aniline/methylpyridine (*m/z* 93), have a weak positive influence from the puff number. Substances occurring at the lower right corner are reactive species such as cyclopentadiene (*m/z* 66) and propyne (*m/z* 40). Their yields are slightly enhanced by the inert atmosphere. Compounds shown at the lower left region (towards air atmosphere) are oxidised hydrocarbons like methylbutanal (*m/z* 86) and acetaldehyde (*m/z* 44).

Discussion

Previous work [13, 53] has established that, when a cigarette is puffed, combustion products formed in the combustion and pyrolysis/distillation zones travel through the bed of unburnt tobacco and the cigarette filter before leaving the cigarette as mainstream smoke. Condensable compounds accumulate downstream from the cigarette coal to form the particulates in cigarette smoke which can be filtered by the unburnt tobacco and filter material. Compounds deposited onto the tobacco in previous puffs can subsequently be re-volatilised by the approaching cigarette coal. This results on a puff-by-puff basis in an increase in the per-puff yield of particulate constituents as the puff number increases. In the cigarette smoking simulator, the presence of the quartz tube prevents air from entering through the paper which dilutes the smoke compounds, and hence a reduced puff-by-puff increase can be expected in these experiments. In this study, an increase in puff-by-puff yields was observed with 2-(4-pyridyl)furan/2,3-dimethyl-1H-indole/3-ethylindole (*m/z* 145) and pyrrole (*m/z* 67) in the cigarette smoking simulator. These compounds can be generated from polymers, proteins or small molecules and are Maillard reaction products [58]. Pyrrole originates from proteins, individual amino acids, alkaloids and nitrates as a pyrolysis product [36].

Ammonia displays an even stronger dependence on the puff number. As ammonia is a gaseous compound, it is not likely to be mechanically filtered in the same way as particulate smoke constituents. However, ammonia is highly water-soluble (520 g/l at 20 °C [59]); therefore, filtration by the tobacco rod may occur due to the moisture content of the tobacco rod. Tobacco moisture increases towards later puffs, due to cumulative condensation of water in smoke onto the tobacco rod, hence promoting more ammonia to be absorbed onto the tobacco surface. In the final puffs, when the remaining unburnt tobacco rod is relatively small, the combination of heat from the burning zone, drying of the remaining tobacco and diminished tobacco filtration can result in a substantial increase in the ammonia yield [57]. The main sources of ammonia in smoke are thought to be

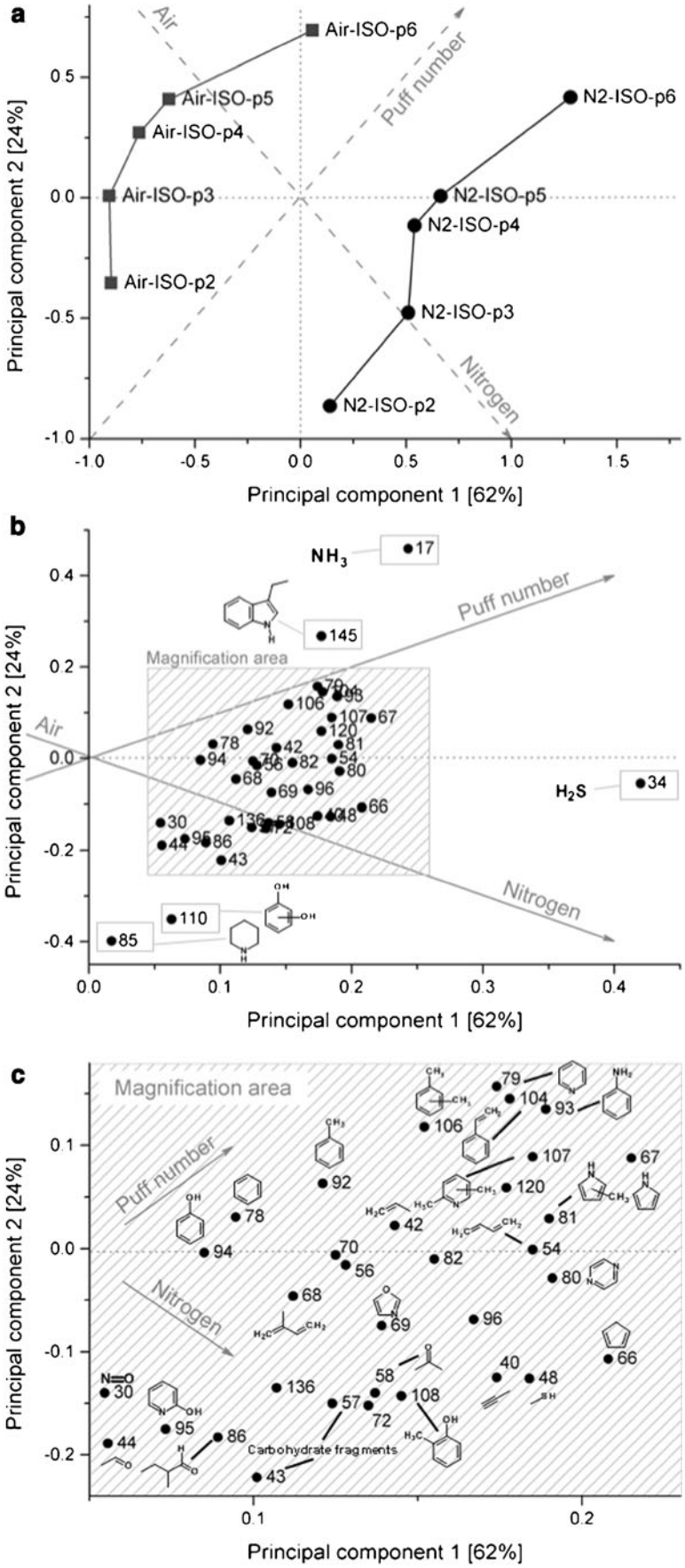

Fig. 5 **a** Score plot of principal component 1 (PC1) and PC2 based on averaged puffs (numbers 2 to 6) from ten 3R4F cigarettes (SI normalised to maximum); **b** loading plot; **c** loading plot (sectional enlargement)

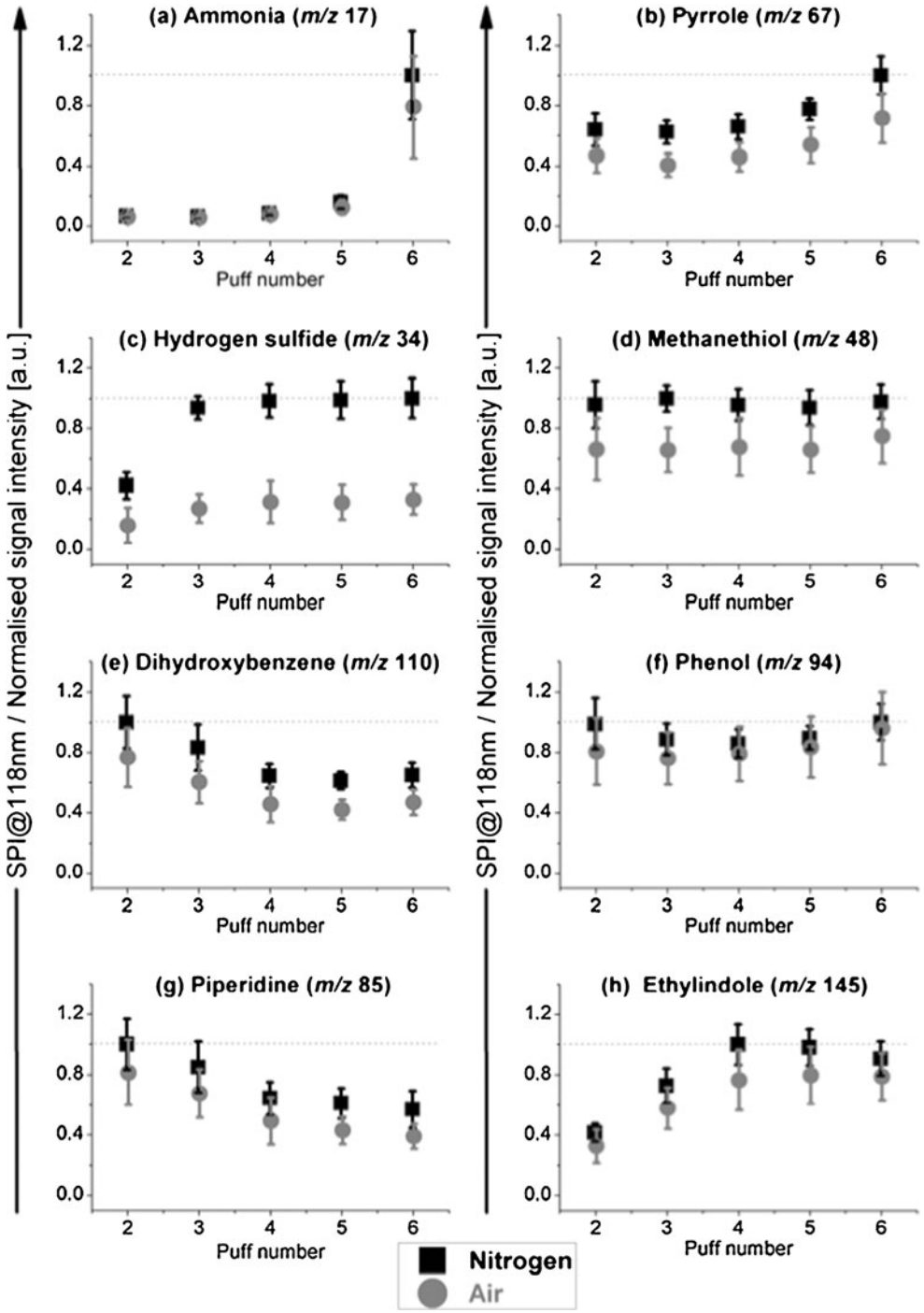

Fig. 6 Mean signal intensity of **a** ammonia (*m/z* 17), **b** pyrrole (*m/z* 67), **c** hydrogen sulphide (*m/z* 34), **d** methanethiol (*m/z* 48), **e** dihydroxybenzene (*m/z* 110), **f** phenol (*m/z* 94), **g** piperidine (*m/z* 85) and (**h**) ethylindole (*m/z* 145) of ten smoked 3R4F cigarettes under nitrogen (*black squares*) and air (*gray circles*) atmosphere (maximum normalised)

the decomposition products from proteins, individual amino acids, alkaloids and nitrates [11, 36]. The lack of sensitivity of ammonia yields to the type of atmosphere suggests that ammonia is released in the pyrolysis zone of the cigarette, where the cigarette is highly depleted in oxygen.

The puff-by-puff yields of detected phenol (*m/z* 94) are constant under a nitrogen atmosphere and increase slightly with an air atmosphere, respectively. This is consistent with the volatile nature of phenol in smoke, which would mean it is less subject to mechanical filtration and subsequent re-evaporation with unburnt tobacco than the tobacco smoke particles. There is little atmospheric sensitivity in the phenol yields. The main precursor compounds for phenol are reported to be chlorogenic acid and lignin, and for diphenols, chlorogenic acid, caffeic acid, rutin, quercetin and lignin as well as cellulose and sugars [11]. It is likely that these decomposition reactions take place in the pyrolysis/distillation zone of the tobacco rod where atmospheric sensitivity can be anticipated to be low.

In contrast to phenol, the amount of detected dihydroxybenzenes (*m/z* 110) and piperidine decrease with increasing

puff number. This phenomenon has been reported previously with formaldehyde and some other volatile materials where the highest yields were observed in the first puff of cigarette smoking [17, 19, 34]. This unusual puff profile has been explained on the basis of the atypical temperature history of the tobacco rod in the initial puffs of the cigarette and implies a relatively low temperature source for these compounds. During pyrolysis of chlorogenic acid, diphenols are formed as primary products from quinic acid and caffeic acid at low temperatures by dehydration and decomposition reactions. Further reactions involving the primary products lead to so-called secondary products such as water, CO_2 and phenol [60]. It was found that an increasing oxygen level during pyrolysis at low temperatures led to a significant decrease of the generated dihydroxybenzenes, but the yields of phenol (i.e., primary decomposition products of tobacco as well as a decomposition product of the residual solid after the tobacco's temperature treatment (350 °C)) were unaffected; therefore, only the decomposition pathways of the dihydroxybenzenes' precursors are influenced by oxygen [61].

The formation of hydrogen sulphide shows a remarkable dependency on puff and atmosphere, with a flat puff-profile in air and with the nitrogen atmosphere an initial rise after the second puff to a flat puff-profile. A satisfactory explanation to this profile and to its different shape compared with methanethiol's profile cannot be provided in this paper and needs further studies.

Finally, it needs to be noted that nearly all substances, such as carbonyl and carboxyl compounds, (poly-) aromatics, heterocyclics and S-/N-containing compounds, feature higher signal intensities under the inert (N_2) condition. A likely explanation for this observation is that an oxidative atmosphere leads to a further degradation of these compounds towards small molecules such as CO, CO_2, H_2O, NOx and HCN [62].

Conclusions

The hyphenation of SPI-TOFMS and the cigarette smoking simulator together with the applied statistical methods have been evaluated and found to be a useful tool that allows investigation of tobacco's thermochemical reactions outside of from natural restrictions present with cigarette smoking (e.g. the necessary presence of oxygen). However, the possibility to compare the results with other findings from different analytical methods is not abandoned. The results presented in this paper reveal that the change of the gas atmosphere—from inert to oxidative conditions—for simulated smoking of 3R4F reference cigarettes lead to a decrease of nearly all compounds' yields but only to small changes in the overall pattern of smoke constituent yields. This observation is in agreement with previous studies which show that majority of the mainstream smoke components are produced by pyrolysis and distillation processes, which are relatively independent of the gas atmosphere. Therefore, yields of substances like benzene and phenol are not influenced significantly due to the mutual dependency of the pyrolysis/distillation zone and the combustion zone in a burning cigarette. Of the compounds examined, the yield of one substance, in particular, hydrogen sulphide, appears to be significantly dependent on the type of atmosphere.

Future work with this system will explore the cigarette smoking simulator's capability to change the puffing and smouldering temperatures for further investigation of the formation mechanisms for smoke constituents. Additional inclusion of REMPI-TOFMS analysis will allow extension of the group of accessible compounds to polycyclic aromatic compounds.

References

1. Paine JB, Pithawalla YB, Naworal JD, Thomas CE (2007) Carbohydrate pyrolysis mechanisms from isotopic labeling. Part 1: the pyrolysis of glycerin: discovery of competing fragmentation mechanisms affording acetaldehyde and formaldehyde and the implications for carbohydrate pyrolysis. J Anal Appl Pyrolysis 80:297–311
2. Paine JB, Pithawalla YB, Naworal JD (2008) Carbohydrate pyrolysis mechanisms from isotopic labeling. Part 3. The Pyrolysis of D-glucose: formation of C-3 and C-4 carbonyl compounds and a cyclopentenedione isomer by electrocyclic fragmentation mechanisms. J Anal Appl Pyrolysis 82(1):42–69
3. Paine JB, Pithawalla YB, Naworal JD (2008) Carbohydrate pyrolysis mechanisms from isotopic labeling. Part 2. The pyrolysis of D-glucose: general disconnective analysis and the formation of C-1 and C-2 carbonyl compounds by electrocyclic fragmentation mechanisms. J Anal Appl Pyrolysis 82(1):10–41
4. Paine JB, Pithawalla YB, Naworal JD (2008) Carbohydrate pyrolysis mechanisms from isotopic labeling Part 4. The pyrolysis of D-glucose: the formation of furans. J Anal Appl Pyrolysis 83(1):37–63
5. Hosoya T, Kawamoto H, Saka S (2007) Pyrolysis behaviors of wood and its constituent polymers at gasification temperature. J Anal Appl Pyrolysis 78(2):328–336
6. Feng JW, Zheng SK, Maciel GE (2004) EPR investigations of charring and char/air interaction of cellulose, pectin, and tobacco. Energy Fuel 18(2):560–568
7. Alen R, Kuoppala E, Oesch P (1996) Formation of the main degradation compound groups from wood and its components during pyrolysis. J Anal Appl Pyrolysis 36(2):137–148
8. Blasi CD (2008) Modeling chemical and physical processes of wood and biomass pyrolysis. Prog Energy Combust Sci 34:47–90
9. Branca C, Giudicianni P, Di Blasi C (2003) GC/MS characterization of liquids generated from low-temperature pyrolysis of wood. Ind Eng Chem Res 42(14):3190–3202
10. Adam T, Streibel T, Mitschke S, Mühlberger F, Baker RR, Zimmermann R (2005) Application of time-of-flight mass spectrometry with laser-based photoionization methods for analytical pyrolysis of PVC and tobacco. J Anal Appl Pyrolysis 74:454–464
11. Rodgman A, Perfetti TA (2009) The chemical components of tobacco and tobacco smoke. Taylor and Francis Ltd, Boca Raton

12. Green CR, Rodgman A (1996) The tobacco chemists' research conference: a half century of advances in analytical methodology of tobacco and its products. Recent Adv Tob Sci 22:131–304
13. Liu C, Feng S, van Heemst J, McAdam KG (2010) New insights into the formation of volatile compounds in mainstream cigarette smoke. Anal Bioanal Chem 396(5):1817–1830
14. Thomas CE, Koller KB (2001) Puff-resolved mainstream smoke analysis by multiplex GC-MS. Beiträge zur Tabakforschung Int/Contrib Tob Res 19(7):345–351
15. Li S, Olegario RM, Banyasz JL, Shafer KH (2003) Gas chromatography-mass spectrometry analysis of polycyclic aromatic hydrocarbons in single puff of cigarette smoke. J Anal Appl Pyrolysis 66(1–2):155–163
16. Wagner KA, Finkel NH, Fossett JE, Gillman IG (2005) Development of a quantitative method for the analysis of tobacco-specific nitrosamines in mainstream cigarette smoke using isotope dilution liquid chromatography/electrospray ionization tandem mass spectrometry. Anal Chem 77(4):1001–1006
17. Xie JP, Yin J, Sun SH, Xie FW, Zhang X, Guo YL (2009) Extraction and derivatization in single drop coupled to MALDI-FTICR-MS for selective determination of small molecule aldehydes in single puff smoke. Anal Chim Acta 638(2):198–201
18. Parrish ME, Lyons-Hart JL, Shafer KH (2001) Puff-by-puff and intrapuff analysis of cigarette smoke using infrared spectroscopy. Vib Spectrosc 27(1):29–42
19. Li S, Banyasz JL, Parrish ME, Lyons-Hart J, Shafer KH (2002) Formaldehyde in the gas phase of mainstream cigarette smoke. J Anal Appl Pyrolysis 65(2):137–145
20. Baren RE, Parrish ME, Shafer KH, Harward CN, Quan S, Nelson DD, McManus JB, Zahniser MS (2004) Quad quantum cascade laser spectrometer with dual gas cells for the simultaneous analysis of mainstream and sidestream cigarette smoke. Spectrochimica Acta Part A-Mol Biomol Spectrosc 60(14):3437–3447
21. Parrish ME, Crawford DR, Gee DL, Harward CN (2007) Intra-puff CO and CO2 measurements of cigarettes with iron oxide cigarette paper using quantum cascade laser spectroscopy. Spectrochim Acta A Mol Biomol Spectrosc 67(1):4–15
22. Shorter JH, Nelson DD, Zahniser MS, Parrish ME, Crawford DR, Gee DL (2006) Measurement of nitrogen dioxide in cigarette smoke using quantum cascade tunable infrared laser differential absorption spectroscopy (TILDAS). Spectrochimica Acta Part A-Mol Biomol Spectrosc 63(5):994–1001
23. Parrish ME, Thweatt WD, Harward CN Sr (2007) Measurement of acrolein and 1,3-butadiene in a single puff of cigarette smoke using lead-salt tunable diode laser infrared spectroscopy. Spectrochimica Acta, part A (Mol Biomol Spectrosc):16–24
24. Schramm S, Carre V, Scheffler JL, Aubriet F (2011) Analysis of mainstream and sidestream cigarette smoke particulate matter by laser desorption mass spectrometry. Anal Chem 83(1):133–142
25. Perfetti TA, Rodgman A (2011) The complexity of tobacco and tobacco smoke. Beiträge zur Tabakforschung Int/ContribTob Res 24(5):215–232
26. Cao L, Muhlberger F, Adam T, Streibel T, Wang HZ, Kettrup A, Zimmermann R (2003) Resonance-enhanced multiphoton ionization and VUV-single photon ionization as soft and selective laser ionization methods for on-line time-of-flight mass spectrometry: investigation of the pyrolysis of typical organic contaminants in the steel recycling process. Anal Chem 75(21):5639–5645
27. Mühlberger F, Hafner K, Kaesdorf S, Ferge T, Zimmermann R (2004) Comprehensive on-line characterization of complex gas mixtures by quasi-simultaneous resonance-enhanced multiphoton ionization, vacuum-UV single-photon ionization, and electron impact ionization in a time-of-flight mass spectrometer: setup and instrument characterization. Anal Chem 76(22):6753–6764
28. Adam T, Ferge T, Mitschke S, Streibel T, Baker RR, Zimmermann R (2005) Discrimination of three tobacco types (Burley, Virginia and Oriental) by pyrolysis single-photon ionisation-time-of-flight mass spectrometry and advanced statistical methods. Anal Bioanal Chem 381(2):487–499
29. Mitschke S, Adam T, Streibel T, Baker RR, Zimmermann R (2005) Application of time-of-flight mass spectrometry with laser-based photoionization methods for time-resolved on-line analysis of mainstream cigarette smoke. Anal Chem 77(8):2288–2296
30. Adam T, Mitschke S, Streibel T, Baker RR, Zimmermann R (2006) Puff-by-puff resolved characterisation of cigarette mainstream smoke by single photon ionisation (SPI)-time-of-flight mass spectrometry (TOFMS): comparison of the 2R4F research cigarette and pure Burley, Virginia, Oriental and Maryland tobacco cigarettes. Anal Chim Acta 572(2):219–229
31. Adam T, Mitschke S, Streibel T, Baker RR, Zimmermann R (2006) Quantitative puff-by-puff-resolved characterization of selected toxic compounds in cigarette mainstream smoke. Chem Res Toxicol 19(4):511–520
32. Adam T, Baker RR, Zimmermann R (2007) Investigation, by single photon ionisation (SPI)-time-of-flight mass spectrometry (TOFMS), of the effect of different cigarette-lighting devices on the chemical composition of the first cigarette puff. Anal Bioanal Chem 387(2):575–584
33. Hanley L, Zimmermann R (2009) Light and molecular ions: the emergence of vacuum UV single-photon ionization in MS. Anal Chem 81(11):4174–4182
34. Adam T, Baker RR, Zimmermann R (2007) Characterization of puff-by-puff resolved cigarette mainstream smoke by single photon ionization-time-of-flight mass spectrometry and principal component analysis. J Agric Food Chem 55:2055–2061
35. Zimmermann R, Dorfner R, Kettrup A (1999) Direct analysis of products from plant material pyrolysis. J Anal Appl Pyrolysis 49:257–266
36. Davis D, Nielsen MT (1999) Tobacco: production, chemistry, and technology. Wiley-Blackwell, Oxford
37. Adam T (2006) Investigation of tobacco pyrolysis gases and puff-by-puff resolved cigarette smoke by single photon ionisation (SPI)–time-of flight mass spectrometry (TOFMS). Ph.D. thesis, Technische Universität München
38. KTRDC (2008) Final FTC smoking results. University of Kentucky. http://www.ca.uky.edu/refcig/3R4F%20Preliminary%20Analysis.pdf
39. Intorp M, Purkis S (2011) Determination of Selected Volatiles in Cigarette Mainstream Smoke. The CORESTA 2008 Joint Experiment. Beiträge zur Tabakforschung Int/Contrib Tob Res 24 (4):174–186
40. Intorp M, Purkis SW, Wagstaff W (2011) Determination of selected volatiles in cigarette mainstream smoke. The CORESTA 2009 Collaborative Study and Recommended Method. Beiträge zur Tabakforschung Int/Contrib Tob Res 24(5):243–251
41. Baker RR (2002) The development and significance of standards for smoking-machine methodology. Beiträge zur Tabakforschung Int/Contrib Tob Res 20:23–41
42. Baker RR (1975) Temperature variation within a cigarette combustion coal during the smoking cycle. High Temp Sci 7:236–247
43. Baker RR (1981) Variation of the gas formation regions within a cigarette combustion coal during the smoking cycle. Beiträge zur Tabakforschung Int/Contrib Tob Res 11(1):1–17
44. Baker RR (1977) Combustion and thermal-decomposition regions inside a burning cigarette. Combust Flame 30(1):21–32
45. Robinson DP, Bevan JL, Weeks AWE (1985) Report: development of a video based burn rate monitor (BRM). BAT Group Research and Development http://legacy.library.ucsf.edu/tid/scd28a99
46. Hicks DR, Wanna JT (2004) Patent: apparatus for making cigarette with burn rate modification. USA Patent US 6,705,325

47. Miura K, Kitao S, Egashira Y, Nishiyama N, Ueyama K (2001) Propagation of cigarette static burn. Beiträge zur Tabakforschung Int/Contrib Tob Res 19(6):277–287
48. Liu C, Woodcock D (2002) Observing the peripheral burning of cigarettes by an infrared technique. Beiträge zur Tabakforschung Int/Contrib Tob Res 20(4):257–264
49. Mitschke S (2007) Application of modern on-line and off-line analytical methods for tobacco and cigarette mainstream and sidestream smoke characterisation Ph.D. thesis, Technische Universität München
50. Eschner MS, Selmani I, Groger TM, Zimmermann R (2011) Online comprehensive two-dimensional characterization of puff-by-puff resolved cigarette smoke by hyphenation of fast gas chromatography to single-photon ionization time-of-flight mass spectrometry: quantification of hazardous volatile organic compounds. Anal Chem 83(17):6619–6627
51. Danzer K, Hobert H, Fischbacher C (2001) Chemometrik: Grundlagen und Anwendungen. Springer, Berlin
52. Einax JW, Zwanziger HW, Geiß S (1997) Chemometrics in environmental analyis. Wiley-VCH, Weinheim
53. Adam T, Mitschke S, Baker RR (2009) Investigation of tobacco pyrolysis gases and puff-by-puff resolved cigarette smoke by single photon ionisation (SPI)–time-of-flight mass spectrometry (TOFMS). Beiträge zur Tabakforschung Int/Contrib Tob Res 23(4):203–226
54. Stedman RL (1968) Chemical composition of tobacco and tobacco smoke. Chem Rev 68(2):153–207
55. Chen PX, Moldoveanu SC (2003) Mainstream smoke chemical analyses for 2R4F Kentucky Reference Cigarette. Beiträge zur Tabakforschung Int/Contrib Tob Res 20(7):448–458
56. Plunkett S, Parrish ME, Shafer KH, Nelson D, Shorter J, Zahniser M (2001) Time-resolved analysis of cigarette combustion gases using a dual infrared tunable diode laser system. Vib Spectrosc 27(1):53–63
57. Shi Q, Nelson DD, McManus JB, Zahniser MS, Parrish ME, Baren RE, Shafer KH, Harward CN (2003) Quantum cascade infrared laser spectroscopy for real-time cigarette smoke analysis. Anal Chem 75(19):5180–5190
58. Serban CM (1998) Chapter 16. Analytical pyrolysis of plant materials. In: Techniques and instrumentation in analytical chemistry, Bd Volume 20. Elsevier, S 441–470
59. Steinbrecht K ((as at) 10 December 2011) Thieme RÖMPP Online: Ammoniak. Georg Thieme Verlag KG. http://www.roempp.com/prod/ (keyword: Ammoniak)
60. Sharma RK, Fisher TS, Hajaligol MR (2002) Effect of reaction conditions on pyrolysis of chlorogenic acid. J Anal Appl Pyrolysis 62(2):281–296
61. McGrath TE, Brown AP, Meruva NK, Chan WG (2009) Phenolic compound formation from the low temperature pyrolysis of tobacco. J Anal Appl Pyrolysis 84(2):170–178
62. Senneca O, Ciaravolo S, Nunziata A (2007) Composition of the gaseous products of pyrolysis of tobacco under inert and oxidative conditions. J Anal Appl Pyrolysis 79(1–2):234–243